

## Supplementary Information for

# A simple integrated design and manufacturing by electrospinning for stabilized lithium battery tin-based anodes

Jiaxin Li<sup>ab</sup>, Mingzhong Zou<sup>b</sup>, Yi Zhao<sup>a</sup>, Zhigao Huang<sup>b\*</sup>, Lunhui Guan<sup>a\*</sup>

<sup>a</sup>Fujian Institute of Research on the Structure of Matter, Chinese Academy of Sciences, Fuzhou 350002, China

<sup>b</sup>College of Physics and Energy, Fujian Normal University, Fuzhou, 350007, China

\*Telephone/Fax: 86-591-83792835. E-mail: guanlh@fjirsm.ac.cn, zg Huang@fjnu.edu.cn.

## Experimental Part

### *Materials synthesis*

Experimentally, all chemicals were of analytical grade and used as received. The samples in this work were all prepared by an electrospinning method based on the previous studies.<sup>[1-3]</sup> Typically, 2.5 g of polyacrylonitrile (PAN,  $M_w$  about 150 000) was dissolved in 25 ml of N, N-dimethylformamide (DMF), and then 1.70 g of  $\text{SnCl}_2 \cdot 2\text{H}_2\text{O}$  and 0.80g  $\text{Cu}(\text{NO}_3)_2 \cdot 3\text{H}_2\text{O}$  were added to form a mixed solution. After vigorous stirring for 40 h at 60 °C, a sticky sol was obtained. For comparison, 25 ml of DMF solution containing 2.5 g PAN was also prepared without adding metal salts. A high voltage power supply was used to provide a 15 kV high voltage for the as-prepared electrospinning solutions. The feed speed rate and needle-to-collector distance were set up at 0.6 ml h<sup>-1</sup> and 15 cm, respectively. The PAN nanofibers were collected on a self-manufactured collector, and then dried for 24 h in vacuum at 80 °C. The dried nanofibers were further stabilized in air at 260 °C for 3 h with a heating rate of 2 °C min<sup>-1</sup>. Finally, the stabilized nanofibers were annealed in a Ar flow at 830

°C for 1 h with a heating rate of 2 °C min<sup>-1</sup> for forming N-doping carbon nanofibers (N-CNFs). N-CNFs loaded with SnCu/SnO<sub>x</sub> material was also prepared by the same process. Finally, the annealed products were obtained as self-standing paper. The self-standing N-CNF paper was cut into disks ( $\phi = 1.25$  cm,  $wt = 1.7 \sim 2.1$  mg), which were directly used as electrodes. These self-standing N-CNF paper electrodes were denoted as N-CNF-PE.

### ***Materials Characterization***

The structures and morphology of these samples were characterized by X-ray diffraction (XRD, RIGAKU SCXmini), X-ray photoelectron spectroscopy (XPS, VG Scientific ESCALAB MK II), Raman Spectra (Renishaw, excited at 514.5 nm), scanning electron microscope (SEM, JSM-6700F) transmission electron microscope (TEM, Tecnai G2 F20), CHNOS Elemental Analyzer (Vario MICRO) and inductively coupled plasma atomic emission spectrometer (ICP-AES, Ultima2).

### ***Electrochemical measurements***

The electrochemical behaviors were measured via CR2025 coin-type cells assembled in a dry argon-filled glove box. The cell consisted of N-CNF-PE and lithium sheet cathode which were separated by a Celgard 2300 membrane and electrolyte of 1 M LiPF<sub>6</sub> in EC:EMC:DMC (1:1:1 in volume). The cells were cycled by LAND2001A at room temperature. Cyclic voltammetry (CV) tests were performed on a CHI660D Electrochemical Workstation with scan rates of 0.1 and 0.5 m Vs<sup>-1</sup>.

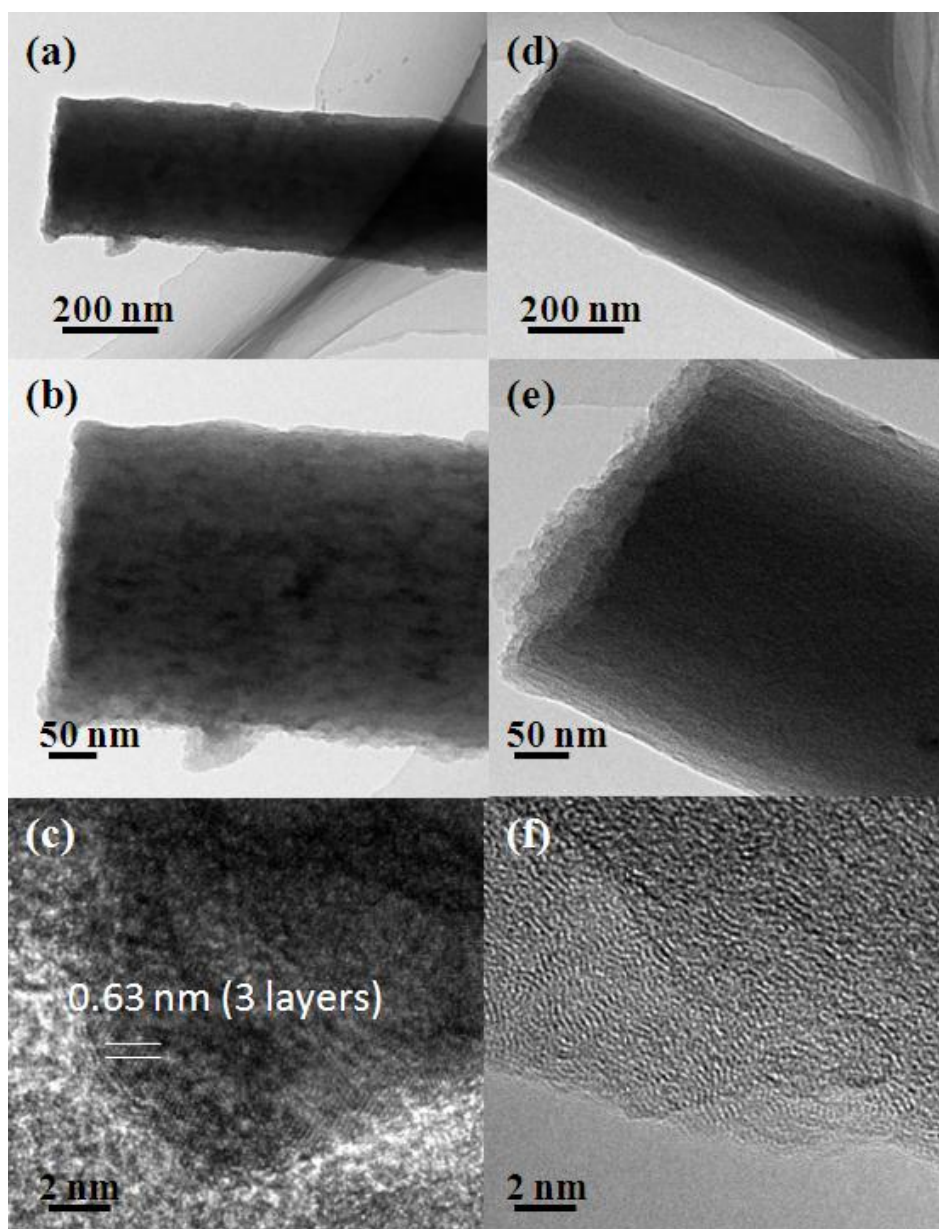


**Fig. S1** TEM and high-resolution TEM images of (a)-(c) SnCu/SnO<sub>x</sub> N-CNFs and (d)-(f) pure N-CNFs.

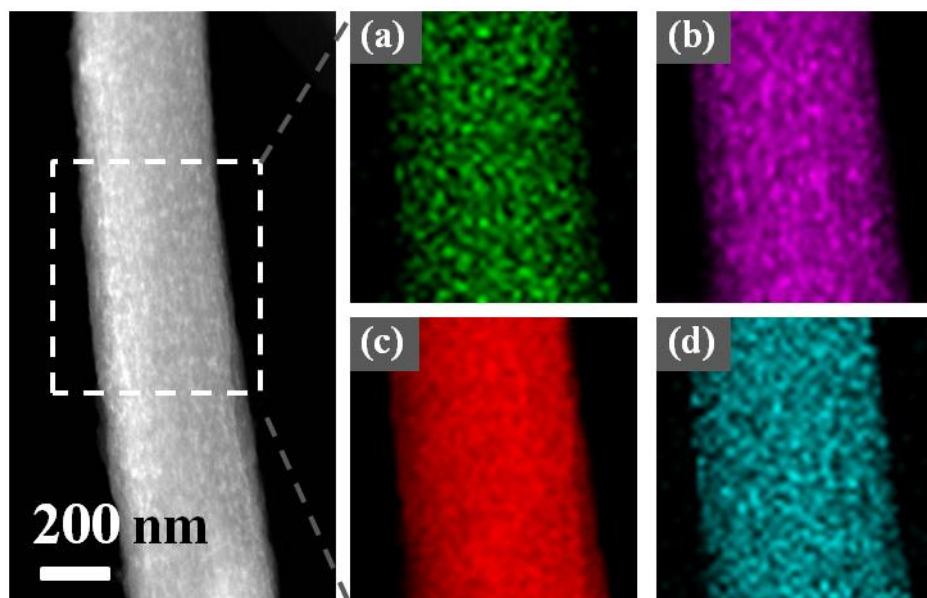


**Fig. S2.** STEM image and (a)O, (b) Sn, (c) C, and (d) Cu element mapping images of as-obtained

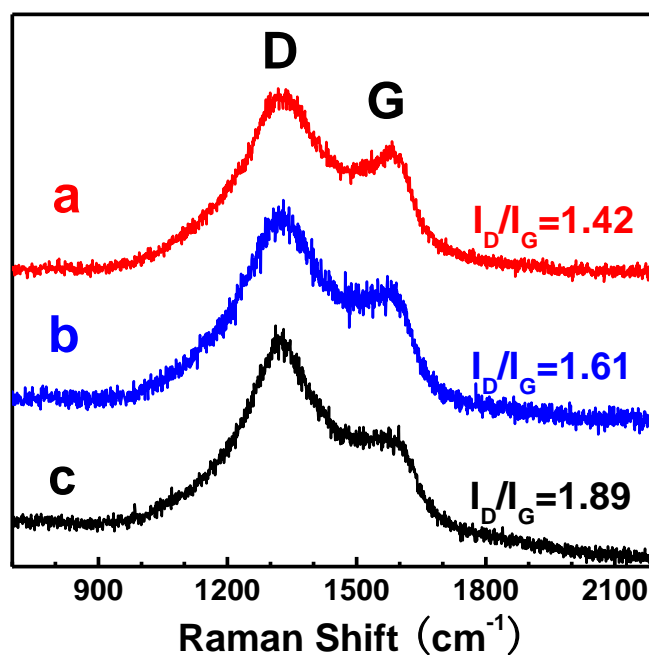


**Fig. S3.** Raman spectra of the (a) without N-doping CNFs derived from PVA(polyvinyl alcohol), (b) pure N-CNFs and (c) SnCu/SnOx N-CNFs with the excitation wavelength of 514.5 nm.

In addition, Raman Spectra is also considered to be a useful technique to detect the N doping in carbon materials. As shown in the **Fig. S3**, Raman results (Renishaw, excited at 514.5 nm) for all samples exhibit the well-known D and G peaks respectively associated with the disordered and graphitized structures, showing the characteristics of microcrystalline graphitic materials. The increasing ratio of the integral intensities  $I_D/I_G$  indicates that the defectiveness of the graphite-like layers grows with increasing of N concentration in the materials. The SnCu/SnO<sub>x</sub> N-CNF sample with the highest N concentration 3.2 wt.% was the most defective. The similar results have also been observed in the previous report.<sup>[4]</sup> Herein, a part of carbon content in the SnCu/SnO<sub>x</sub> N-CNFs has been consumed in the redox reaction, leading to a higher N concentration compared to that of 2.4 wt. % in pure N-CNFs.

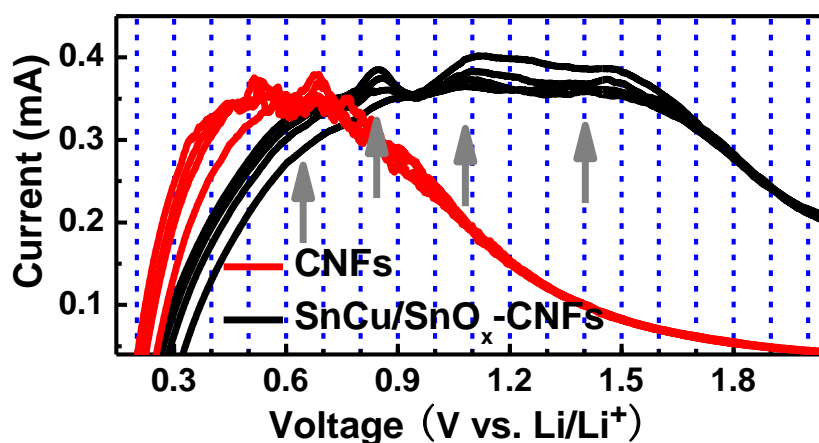


**Fig. S4.** The magnified cyclic voltammetry curves at 0.5 mV/s for N-CNF-PE  
SnCu/SnO<sub>x</sub> N-CNF-PE.

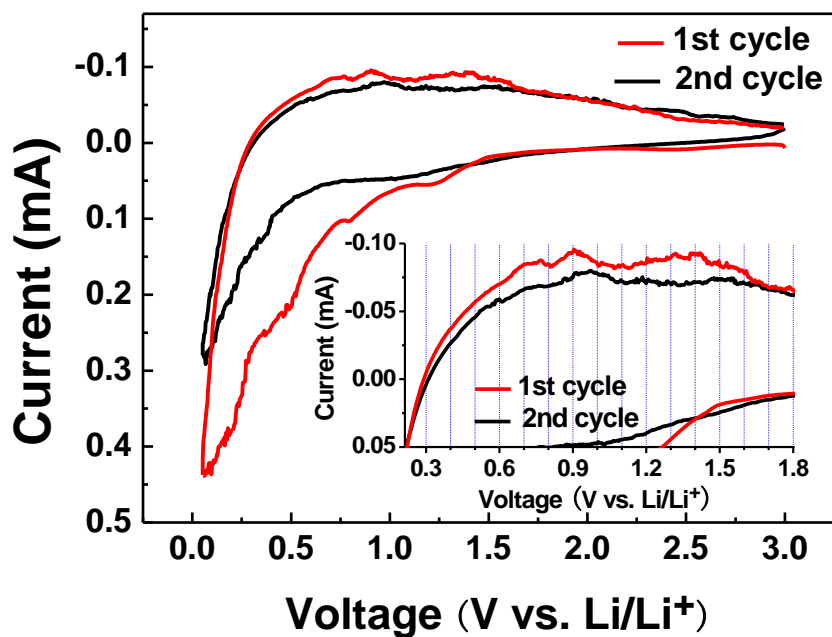


**Fig. S5.** The cyclic voltammetry curves of SnCu/SnO<sub>x</sub> N-CNFs at 0.1 mV/s. The inset is the corresponding magnified cyclic voltammetry curve.

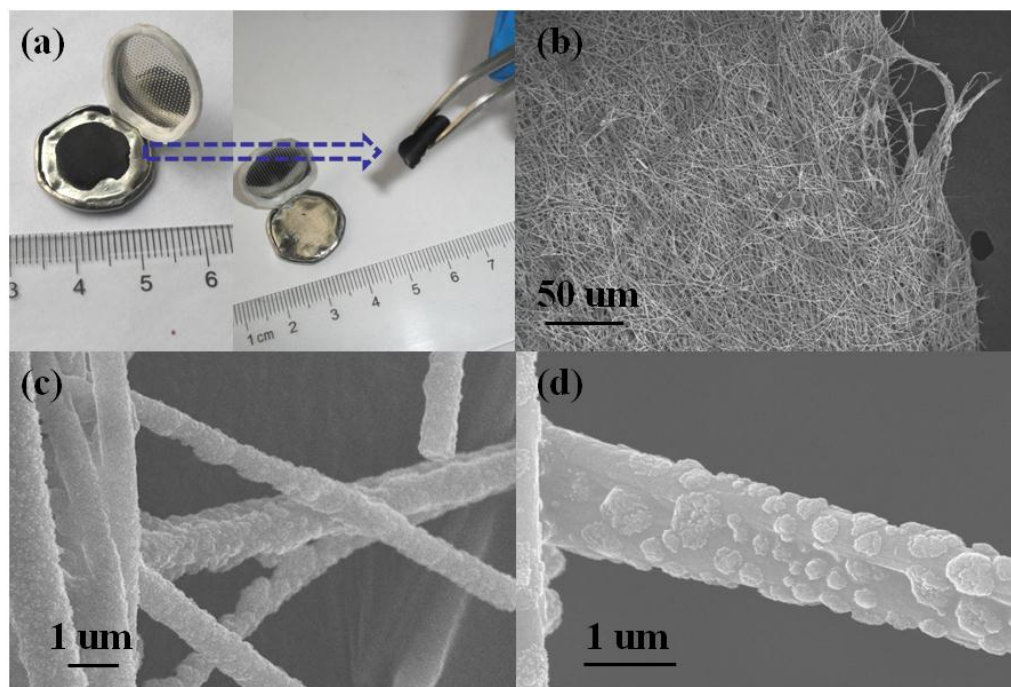


**Fig. S6.** (a), Digital camera images of SnCu/SnO<sub>x</sub> N-CNF-PE after cell test; (b),(c) and (d),The corresponding SEM images of the SnCu/SnO<sub>x</sub> N-CNFs.

## The detailed calculation:

The XPS, Elemental Analyzer and ICP have been used to exactly detect the ratio of Sn, Cu, N, O and C in SnCu/SnO<sub>x</sub> N-CNFs. The contents of Sn, Cu, N, O and C in the SnCu/SnO<sub>x</sub> N-CNFs are 35 wt.%, 10.3 wt.%, 3.2 wt.%, 1.5 wt.% and 50 wt.%, respectively. Herein, we assume that most of O element in SnCu/SnO<sub>x</sub> N-CNFs is from SnO<sub>2</sub>. Accordingly, the Sn and SnO<sub>2</sub> in the SnCu/SnO<sub>x</sub> N-CNFs are about 29.5 wt.% and 7 wt.%. Thus, the capacities of both Sn and SnO<sub>2</sub> are ~343 mA/g [i.e.,  $C - (C_{N-CNFs} * 50 \text{ wt.}\%) = 470 - (255 * 0.50) = 343$ ]. When the specific theoretical capacities of Sn and SnO<sub>2</sub> (994 and 782 mAh g<sup>-1</sup>) were all utilized reversibly, the contribution of Sn and SnO<sub>2</sub> to the SnCu/SnO<sub>x</sub> N-CNFs are about 347 mA/g [i.e.,  $(994 * 29.5 \text{ wt.}\%) + (782 * 7 \text{ wt.}\%) = 347$ ]. Thus, we can know that the capacity of 343 mA/g is close to 347 mA/g, indicating ~100 % of the theoretical capacities of Sn and SnO<sub>2</sub>.

Thus, the reversible capacity of SnCu/SnO<sub>x</sub> embedding in N-CNFs can almost achieve its theoretical capacity under low current densities in this current study. It is concluded that the electrochemical performance of SnCu/SnO<sub>x</sub> N-CNFs can be strongly improved by using this simple integrated design and manufacturing.

## Refs:

- [1] Jang B. O., *et al.*, *J. Alloys Compounds*, **2013**, 574, 325.
- [2] Bonino C. A. *et al.*, *ACS Appl. Mater. Interface.*, **2011**, 3, 2534.
- [3] Jung H. R. *et al.*, *J. Electrochem. Soc.*, **2011**, 158 (6), A644.
- [4] Ismagilov Z. R. *et al.* *Carbon*, **2009**, 47, 1922.